Urban Scale Photovoltaic Charging Stations for Electric Vehicles

Morris Brenna, *Member, IEEE*, Alberto Dolara, *Student Member, IEEE*, Federica Foiadelli, *Member, IEEE*, Sonia Leva, *Senior Member, IEEE*, and Michela Longo

I. Introduction

INFLUENCED by recent developments in the oil market and greater sensitivity in terms of pollutants, the last decade has seen a growing interest in electric mobility. Despite major technological developments in various areas of research, there are still many issues to be addressed. Among these, the need for a reliable and diverse charging infrastructure which meets different user needs is placed at the forefront. In its directive on introduction of renewable energy, the European Parliament states that 20% of the energy use within the union should be covered by renewable energy sources by 2020 [1], [2]. Today, there are several suggested alternatives to fossil fuels that are being well investigated in order to replace fossil fuels in many aspects of human life and industries. Several economical, ecological, and political ambitions lie behind this replacement, one of which is greenhouse gas pollution leading to global warming. A sector mostly involved from this issue is the transportation sector that sees the replacing of a number of conventional internal combustion engine (ICE) vehicles with electric vehicles (EVs) [3].

Through an intelligent integrating of vehicles, electricity, free renewable fuel, and market opportunities, it is possible to make a zero-carbon future. Renewable energy such as photovoltaic (PV) integrated in a vehicle-to-grid (V2G) concept could be a solution to alleviate carbon footprint. An effective way to maximize the utilization of space and capacity of the V2G parking lot (VPL) is the integration of PV rooftops as a micro-resource in the VPL facility [4]. A plug-in hybrid EV (PHEV) is essentially a hybrid vehicle with a larger battery pack [5], [6]. Therefore, it runs on electricity when its battery state-of-charge (SOC) is high. Otherwise, the ICE takes over and the vehicle consumes gasoline similar to a hybrid vehicle. The battery pack can be recharged through a charging station connected to an electric power grid. PHEVs are characterized by their all-electric range (AER). The quantity of electricity demanded by PHEVs raises concerns about their potential negative impacts on the grid. Therefore, it is important to analyze possible alternative solutions to supply the EVs. Considering the wide diffusion of renewable sources, it comes to mind the idea to exploit these energies to help the EVs charging [7], [8]. Other sources can also be considered for charging EVs. For example, in the metropolitan areas, braking energy coming from the urban transportation systems can be exploited for the EVs charge [9].

These studies often refer to scenarios in which renewable solutions benefit of national economical incentives. Recently, due to the economical crisis, these funds have been dramatically reduced, especially in Europe, and therefore, it is important to reach an economical sustainability of the so-called green solutions. A further step is therefore thinking about applications to increase the self-consumption in order to improve the profitability of renewable energy power plants also in the absence of economical incentives. Considering the scientific background, this idea is already under study and development in building applications where the PV production can directly supply building devices as heat pumps or can be stored in dedicated batteries to reach a self-sustainability of the system [10], [11].

This paper addresses to this concern and it analyzes the benefits of integrating a PV carport in the charging station and how to better exploit the available energy. Since most cars used for work purposes remain parked during the day, a common scenario could be to charge PEVs during work hours. The paper focuses on those charging infrastructures dedicated to commuters with access to reserved parking areas at their workplace. Considering an installation having a good

Manuscript received February 27, 2014; revised May 15, 2014; accepted July 19, 2014. Date of publication August 14, 2014; date of current version September 16, 2014.

The authors are with the Department of Energy, Politecnico di Milano, Milano 20133, Italy (e-mail: morris.brenna@polimi.it; alberto.dolara@polimi.it; federica.foiadelli@polimi.it; sonia.leva@polimi.it; michela.longo@polimi.it).

TABLE I
PARAMETERS USED FOR ANALYSIS

Geographical locations	PV technology	Tilt angle (°)	Azimuth angle (°)	Month
North-, Center-, South-Italy	Crystalline silicon, CIS, CdTe, and thin film	0, 5, 10, 15, 20, 25, 30, 35, 40, 45, 50, 55, 60, 65, 70 75, 80, 85, 90	0, ±10, ±20, ±30, ±40, ±50, ±60, ±70, ±80, ±90	1 — Jan. 2 — Feb. 3 — Mar. 4 — Apr. 5 — May 6 — Jun. 7 — Jul. 8 — Aug. 9 — Sep. 10 — Oct. 11 — Nov. 12 — Dec.

availability of space, a good exposure to solar radiation, and a reduced presence of shading [12], an outdoor parking justifies the development of a PV carport in replacement of the traditional shelter. However, the overall efficiency of renewable energy systems requires a high level of optimization of their components [13]. The efficient exploitation of nonprogrammable renewable sources is also related to the accuracy in the forecasting of their production [14]. Finally, the load profile depends on several variables that can be assumed to be stochastically distributed, including actual SOC of the battery, parking duration, parking type, and vehicle powertrain [15]. A statistical approach based on measurements campaign is useful to improve the accuracy in load profile predictions [16].

In this study, a PV charging system has been analyzed. In Section II, a mathematical law that estimates the production from PV shelter as a function of different parameters based on a statistical approach is defined. Section III presents the mathematical model of the system that considers the power flows related to the PV generator, the charging station, and electric grid. Section IV contains details of the proposed charging system, whereas Section V applies the previous analysis.

II. ENERGY PRODUCTION FROM PV SYSTEM

This section presents an energy production estimation of PV systems, considering different factors such as localization, technology, orientation, and period. In particular, three geographical locations in Italy representing different solar radiation levels (north Italy—low solar radiation, center Italy—medium solar radiation, and south Italy—high solar radiation), different orientations of the PV generator (in terms of tilt and azimuth angles), and various PV technologies have been considered. Table I summarizes the values used in this analysis.

The goal of this analysis is to define a mathematical law that allows assessing the production of a PV system as a function of the month and the orientation of the PV generator. In this paper, the regression approach is applied.

The data used to assess the production of the PV systems have been extracted from the database of the software Photovoltaic Geographical Information System (PVGIS) [17], developed by the Joint Research Center, a Directorate General of the European Commission. The outputs provided by the program are based on a climatic database that considers measured data from 2000 to 2009.

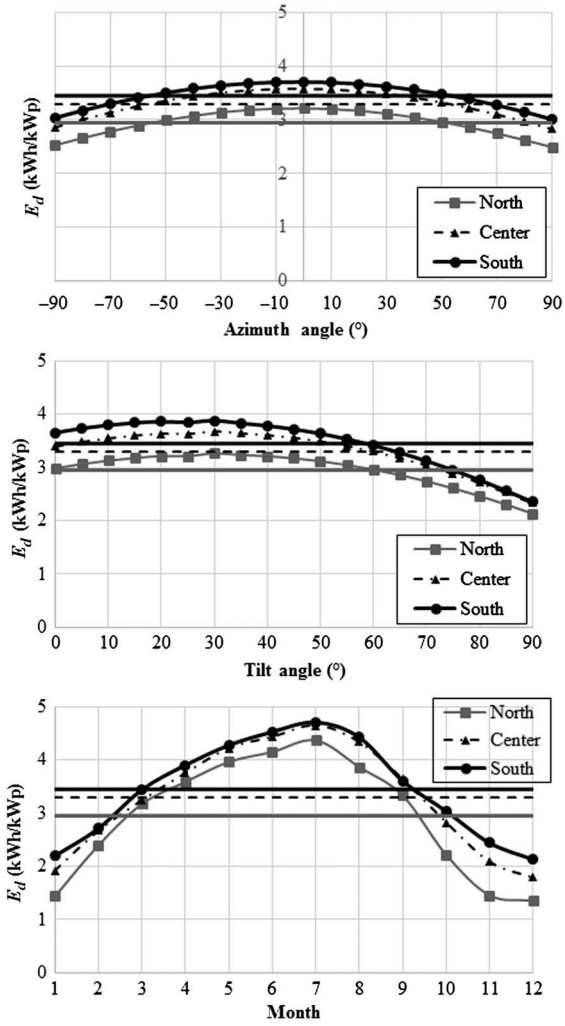

Fig. 1. Daily energy production in different regions of Italy. The horizontal lines represent the average values.

The inputs required by the program are the following.

1) The geographical coordinates of the site.
2) Peak power of PV plant. In this work, a base power of 1 kWp is considered to easily extend the results to PV systems of any peak power.
3) Installation: free-standing.
4) Estimated system losses: 14%.
5) PV technology, azimuth, and tilt angles as reported in Table I.

The outputs of the program are the following.

1) E_d: Average daily electricity production from the given system (kWh).
2) E_m: Average monthly electricity production from the given system (kWh).
3) H_d: Average daily sum of global irradiation per square meter received by the modules of the given system ($\mathrm{kWh/m^2}$).
4) H_m: Average sum of global irradiation per square meter received by the modules of the given system ($\mathrm{kWh/m^2}$).

In particular, in this work only E_d has been considered.

Fig. 1 shows the variation of the daily electricity production E_d as a function of azimuth and tilt angles and installation region.

TABLE II
COEFFICIENTS FOR (1) FOR DIFFERENT PV TECHNOLOGY AND GEOGRAPHICAL AREAS

PV technology	Geographical locations	R^2(%)	k_1 $\left(\frac{\text{kWh}}{\text{kWp}\times\text{deg}^2}\right)$	k_2 $\left(\frac{\text{kWh}}{\text{kWp}\times\text{deg}^2}\right)$	k_3 $\left(\frac{\text{kWh}}{\text{kWp}\times\text{month}^2}\right)$	k_4 $\left(\frac{\text{kWh}}{\text{kWp}\times\text{deg}}\right)$	k_5 $\left(\frac{\text{kWh}}{\text{kWp}\times\text{month}}\right)$	k_6 $\left(\frac{\text{kWh}}{\text{kWp}\times\text{deg}\times\text{month}}\right)$	k_7 $\left(\frac{\text{kWh}}{\text{kWp}}\right)$
Si	North	85.5	-30×10^{-5}	-9×10^{-5}	-97×10^{-3}	15.3×10^{-3}	1.19	29×10^{-5}	0.78
	Center	82.4	-33×10^{-5}	-9×10^{-5}	-91×10^{-3}	15.6×10^{-3}	1.14	39×10^{-5}	1.24
	South	79.4	-35×10^{-5}	-8×10^{-5}	-84×10^{-3}	13.7×10^{-3}	1.04	42×10^{-5}	1.67
CIS	North	85.3	-31×10^{-5}	-9×10^{-5}	-100×10^{-3}	16.0×10^{-3}	1.23	28×10^{-5}	0.74
	Center	82.2	-35×10^{-5}	-9×10^{-5}	-94×10^{-3}	16.6×10^{-3}	1.18	39×10^{-5}	1.20
	South	78.6	-37×10^{-5}	-9×10^{-5}	-86×10^{-3}	15.0×10^{-3}	1.07	43×10^{-5}	1.66
CdTe	North	86.4	-31×10^{-5}	-9×10^{-5}	-112×10^{-3}	15.9×10^{-3}	1.38	28×10^{-5}	0.69
	Center	83.6	-35×10^{-5}	-9×10^{-5}	-105×10^{-3}	16.4×10^{-3}	1.32	38×10^{-5}	1.19
	South	80.2	-37×10^{-5}	-9×10^{-5}	-95×10^{-3}	15.0×10^{-3}	1.20	42×10^{-5}	1.71
Thin film	North	85.8	-31×10^{-5}	-8×10^{-5}	-106×10^{-3}	16.4×10^{-3}	1.31	27×10^{-5}	0.44
	Center	82.4	-35×10^{-5}	-9×10^{-5}	-100×10^{-3}	17.3×10^{-3}	1.26	36×10^{-5}	0.91
	South	79.4	-37×10^{-5}	-8×10^{-5}	-92×10^{-3}	15.6×10^{-3}	1.17	40×10^{-5}	1.37

It is possible to observe that the pairs of tilt and azimuth angles that maximize the energy production are around 30° and 0°, respectively, for all regions. In terms of average value over a year, north of Italy is characterized by the lower value, 2.94 kWh/(kWp·day), whereas south of Italy is characterized by the highest value, 3.45 kWh/(kWp·day), highlighting that the energy production in Italy increases from the North to the South. The PV technologies do not considerably influence the production and the applied method. Therefore, the choice of the crystalline silicon PV technology is based on its diffusion in the installed PV plants.

A general mathematical law to estimate the daily production can be obtained from the analysis of the curves represented in Fig. 1

$$E_d(m,\,T,\,A) = k_1\cdot T^2 + k_2\cdot A^2 + k_3\cdot m^2 + k_4\cdot T + k_5\cdot m + k_6\cdot T\cdot m + k_7 \quad (1)$$

where m is month, T is the tilt in degrees, A is the azimuth in degrees, and k_1, k_2, k_3, k_4, k_5, k_6, and k_7 are weight coefficients. In Table II, the values of the coefficients for the different regions using Minitab software are reported. It is possible to observe that the values of the coefficient of determination (R^2), that indicates how the mathematical model fits the data provided by PVGIS, are quite high.

III. MATHEMATICAL MODEL OF THE POWER FLOWS

The assessment of the energy flows within the charging system requires the knowledge of the daily production curves of the PV system and the demand curves of the EVs.

A first analysis could be based on the annual energy balance. In this case, the average daily energy produced by the PV system could be evaluated by applying the method presented in Section II to PV systems dedicated to the EVs charging systems installed on carports. Usually, these parking areas have a footprint between 10 and 15 m^2 available for each vehicle. Therefore, it is possible to install on their roofs a PV generator that has a peak power between 1.5 and 2.5 kWp/car.

Considering the typical roof pitches of the carports and considering that the average distance travelled annually in urban and suburban areas by the commuters is about 10 000 km and the average energy consumption of an electric vehicle is about 0.2 kWh/km, the annual energy production estimated starting from (1) is comparable to the energy required by EVs. In the worst condition (north of Italy, winter months and both vehicles in charge), it is possible to estimate that 30% of the recharge energy have to be absorbed from the grid. For these reasons, the solar energy can be suitably exploited for charging EVs.

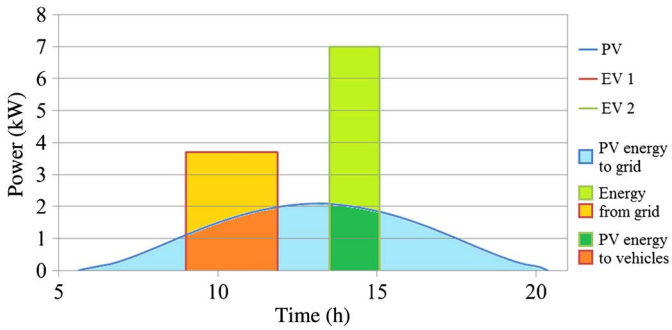

Fig. 2. Example of the noncoordinability of the production curve and load curve.

However, there is a limit in the annual analysis, because the PV production curve (strongly related to the weather conditions) and the load curve (that depends by EV charging and working conditions) do not match.

In this work, the production curve of a PV carport sized for two EVs has been considered. As per load curves, combinations of two different EV typologies are considered: a car (*C*) with battery capacity of 24 kWh and a quadricycle (*Q*) with battery capacity of 9 kWh. Charging power has been assumed constant throughout the charging period.

To assess in detail the potential of PV charging stations, it is necessary to carry out the comparison between these two power curves. Fig. 2 shows an example of the comparison between the charging power curves and the PV production curve in the case of two cars charged sequentially—the first one in the morning and the second one in the afternoon—with the same amount of energy but with different charging powers.

The matching between the two curves cannot be generalized by an equation, but it has to be done analyzing case by case.

For this reason, the following two main scenarios are analyzed as follows.

1) Contemporary charging of two vehicles: Charging begins on arrival at work, at 9:00 A.M.
2) Sequential charging of vehicles: The company organizes shifts for charging EVs, one that starts at 9:00 A.M. and one at 1:30 P.M.

Each scenario considers:

1) Three combinations of EVs: two cars (C1 and C2), a car (*C*) and a quadricycle (*Q*), and two quadricycles (Q1 and Q2).
2) Different values of charging power: 3.7, 7, 11, and 22 kW. However, current market available quadricycles cannot be charged with power exceeding 3.7 kW; therefore, the number of scenarios that contain one or two quads is reduced.
3) The energy that must be provided to the vehicles will depend on the difference between the initial and final states of charge of the battery (ΔSOC). Three values of ΔSOC (0.6, 0.4, and 0.2) will be considered in C1–C2 and *C–Q* combinations. Instead, considering that there is only one available charging power for the quadricycles, five values of ΔSOC (0.6, 0.5, 0.4, 0.3, and 0.2) will be taken in account for the two quadricycles combination in order to increase the number of the cases.

The different combinations give rise to more than 9000 different cases here analyzed.

The evaluation of the energy flows shall be according to the following scheme.

Starting from the combination of vehicles and the difference between the initial and final state of charge ΔSOC and their battery capacity C_{batt}, the energy E_{rech} required in a day to recharge both vehicles *v*1 and *v*2 is obtained

$$E_{\mathrm{rech}} = E_{\mathrm{rech},v1} + E_{\mathrm{rech},v2} = \sum_{v=1}^{2} C_{\mathrm{batt},v} \cdot \Delta\mathrm{SOC}_v. \quad (2)$$

Charging time is calculated considering the charging power P_{rech}, the energy required E_{rech}, and the efficiency of the charging process η_{rech}. In case of contemporary charge, charging time Δt and consequently the initial (t_i) and final (t_f) charging instants are

$$\Delta t = \frac{E_{\mathrm{rech}}}{P_{\mathrm{rech}} \cdot \eta_{\mathrm{rech}}}; \qquad t_f = t_i + \Delta t. \quad (3)$$

In case of sequential charge, charging time for each vehicle is

$$\begin{aligned} \Delta t_1 &= \frac{E_{\mathrm{rech},v1}}{P_{\mathrm{rech},v1} \cdot \eta_{\mathrm{rech}}}; \qquad t_{f,1} = t_{i,1} + \Delta t_1 \\ \Delta t_2 &= \frac{E_{\mathrm{rech},v2}}{P_{\mathrm{rech},v2} \cdot \eta_{\mathrm{rech}}}; \qquad t_{f,2} = t_{i,2} + \Delta t_2. \end{aligned} \quad (4)$$

It is important to note that the charging time of each vehicle has to be always lower than the time slot assigned for its recharge. As a consequence, the vehicle that starts its recharge at 9:00 A.M. reaches the state of full charge before the beginning of the recharge of the second vehicle at 1:30 P.M.

The energy produced by the PV plants during the charging process, called "self-consumption" $E_{\text{self-cons}}$, has been estimated for each month considering the daily average production curve

$$E_{\text{self-cons}} = \int_{t_i}^{t_f} P_{\mathrm{PV}}(t)dt \quad (5)$$

where $P_{\mathrm{PV}}(t)$ is the power produced by the PV system. It can be evaluated by using the monthly average curve to determine the sun–rise and the sun–set and the average daily electricity production from (1).

Equation (5) is applied in all scenarios because the PV generator peak power is always lower than the minimum power required for the recharge. The condition where the energy produced by the PV systems is at the same time supplied to vehicles and to the electric grid never occurs.

Consequently, for every month and every case, the energy to withdraw from the grid E_{grid} to complete the recharge process can be estimated as follows:

$$E_{\mathrm{grid}} = \frac{E_{\mathrm{rech}}}{\eta_{\mathrm{rech}}} - E_{\text{self-cons}}. \quad (6)$$

Finally, the amount of energy produced by the PV system and injected into the grid can be calculated as the difference between the estimated energy produced by the PV system given in (1) and the estimated self-consumption for EVs recharging

$$E_{\mathrm{PV}->\mathrm{grid}} = E_d - E_{\text{self-cons}}. \quad (7)$$

The values so obtained are calculated for each day. The following equations are used for the monthly value:

$$\begin{aligned} E_{\mathrm{rech},m} &= F \cdot n_{\mathrm{day,month}} \cdot E_{\mathrm{rech}} \\ E_{\text{self-cons},m} &= F \cdot n_{\mathrm{day,month}} \cdot E_{\text{self-cons}} \\ E_{\mathrm{grid},m} &= (E_{\mathrm{rech},m} - E_{\text{self-cons},m}) \cdot F \cdot n_{\mathrm{day,month}} \\ E_{\mathrm{PV}->\mathrm{grid},m} &= (E_d - E_{\text{self-cons}}) \cdot F \cdot n_{\mathrm{day,month}}. \end{aligned} \quad (8)$$

where $n_{\mathrm{day,\,month}}$ is the number of days in the considered month.

IV. Details of PV Charging Systems

In this work, the charging system analyzed consists of a charge point for two PEVs that can be supplied from the grid and/or from the PV generator installed on the roof of the carport. In particular, it has been considered as a PV shelter installed in a company car park area where the EVs are available for recharge from 9:00 A.M. to 5:00 P.M.

The PV shelter is designed for two EVs and takes up an area of about $25\ \mathrm{m}^2$. The PV generator is made up by 15 monocrystalline PV modules, for a total power of 3675 Wp. It is assumed that the tilt angle is equal to 20° and azimuth is equal to 0°.

Fig. 3 shows the PV system, the elements of the charging station, and the energy flows. The red arrows represent the flows of energy produced by the PV system, whereas the blue arrows represent the flows of energy drawn from the electric grid. When the energy demand from the user is nil, the energy produced from the PV system is injected into the grid. When one or two EVs are connected to the recharge station, the energy produced by the PV system is completely supplied to

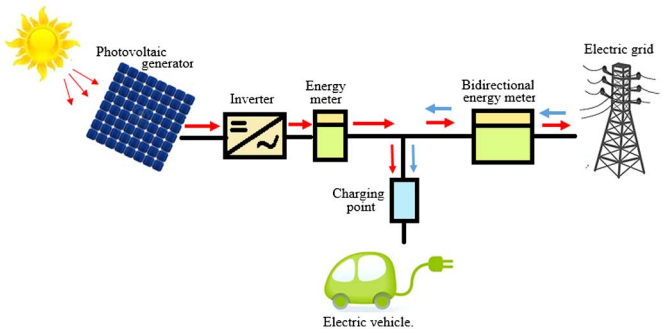

Fig. 3. Power flows of the proposed charging system.

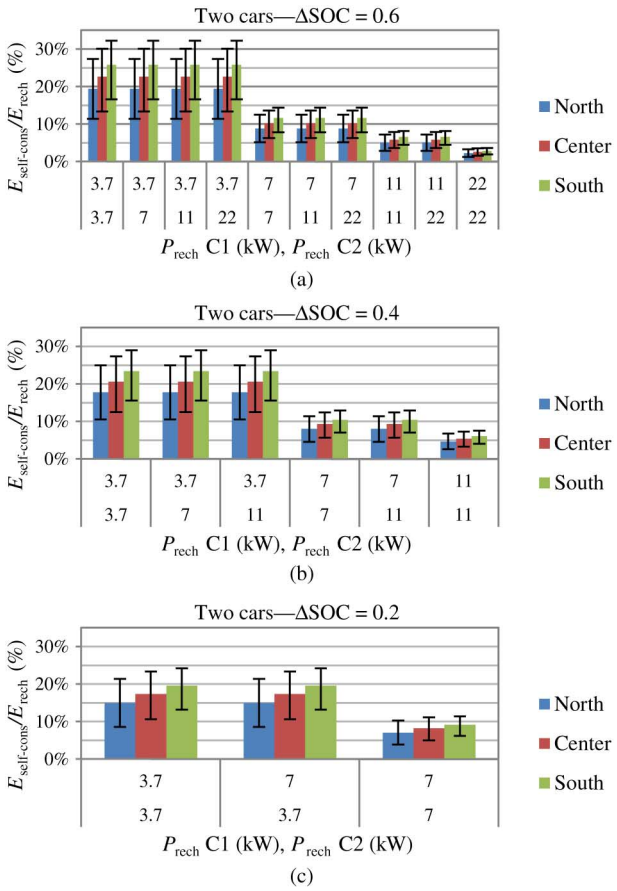

Fig. 4. (a) $\Delta SOC = 0.6$. (b) $\Delta SOC = 0.4$. (c) $\Delta SOC = 0.2$. Contemporary charging of two cars (C1 and C2). The recharge power of car 1 and car 2 are reported on the category axis, starting from the top.

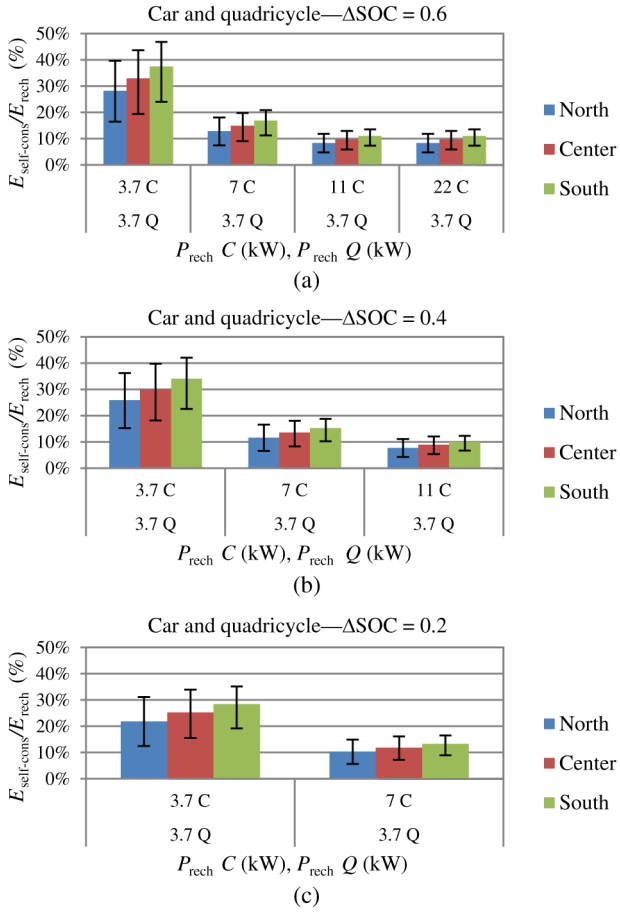

Fig. 5. (a) $\Delta SOC = 0.6$. (b) $\Delta SOC = 0.4$. (c) $\Delta SOC = 0.2$. Contemporary charging of a car (C) and a quadricycle (Q) as a function of ΔSOC. The recharge power of the car (C) and quadricycle (Q) are reported on the category axis, starting from the top.

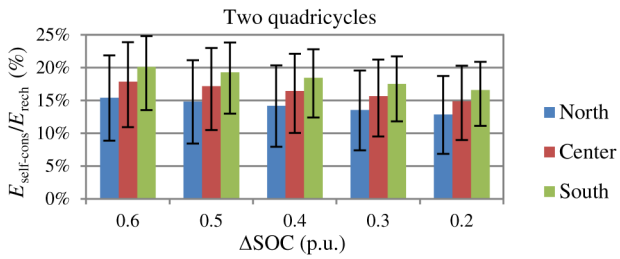

Fig. 6. Contemporary charging of two quadricycles (Q1 and Q2). The ΔSOC of each quadricycle are reported on the category axis.

the onboard batteries. This operating condition is related to the size of PV generator. In fact, its peak power is lower than the minimum power required for the recharge; therefore, it is not possible that the PV system supplies both vehicles and grid.

V. Results and Discussion

This section presents the main results of the analysis in term of the quantification of energy flows into the PV charging stations. Among of the energy flows, the self-consumption $E_{\text{self-cons}}$ is the most important flow; it represents the amount of energy that is produced by the PV charging station that is directly stored in the PEVs batteries.

The evaluation of self-consumption has been made considering several values of ΔSOC, recharge power, combinations of cars (C) and quadricycles (Q), and several sites. Charging powers are chosen as a function of ΔSOC. Taking into account that high charging powers reduces the batteries life they have to be avoided if there is not the need to provide significant amounts of energy. Therefore, the maximum charging power (22 kW) is considered only when the energy that has to be supplied to the batteries is maximum ($\Delta SOC = 0.6$). Charging power of 11 kW is excluded when the energy that has to be supplied to the batteries is the minimum ($\Delta SOC = 0.2$). The ainnual value of $E_{\text{self-cons}}$ is calculated starting from the monthly $E_{\text{self-cons}}$.

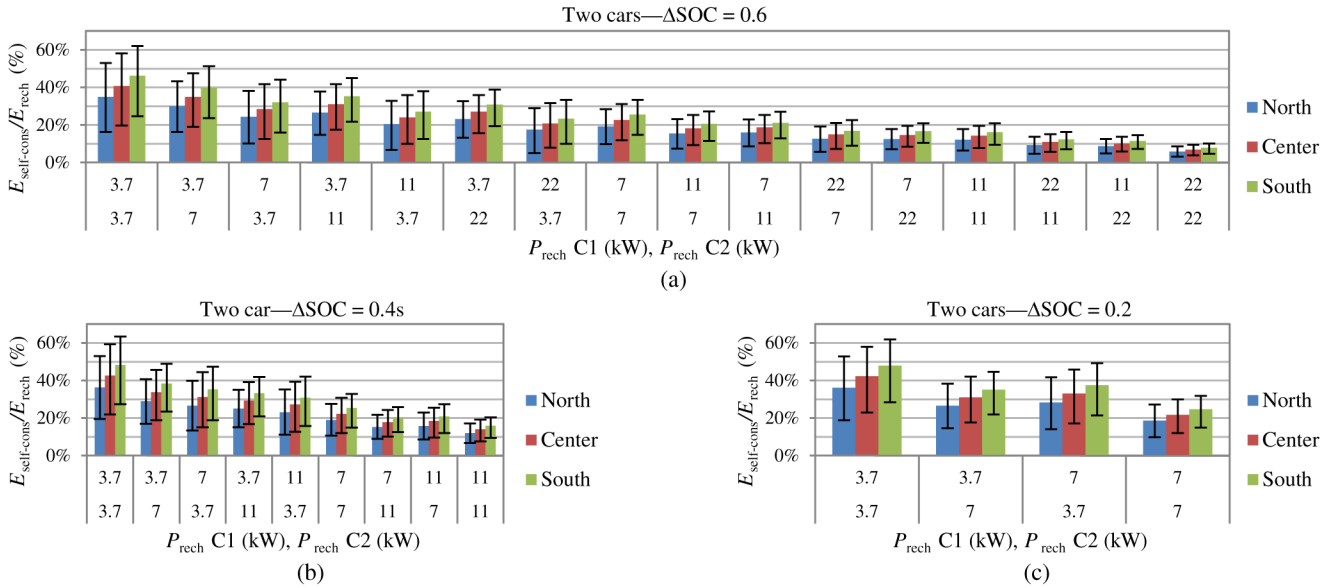

Fig. 7. (a) $\Delta SOC = 0.6$. (b) $\Delta SOC = 0.4$. (c) $\Delta SOC = 0.2$. Sequential charging of two cars. The recharge power of car 1 (C1) and car 2 (C2) are reported on the category axis, starting from the top.

In the following, the annual average, minimum, and maximum value of self-consumed energy are reported. These values are expressed as a percentage of the recharge energy E_{rech} and they are grouped in histograms where the bars indicate the annual value, whereas the error bars indicate the minimum and maximum values achieved in the months of December and June, respectively.

A. Scenario 1: Contemporary Charging

The first set of graphs (Figs. 4–6) shows the results obtained for the contemporary charging scenario. Fig. 4 shows the self-consumption in case of contemporary charge of two cars, considering the values of ΔSOC of 0.6 (case a), 0.4 (case b), and 0.2 (case c) for each car; charge powers taken into account for each car are shown on the category axis.

Fig. 5 shows the self-consumption in case of contemporary charge of a car and a quadricycle, considering the values of ΔSOC of 0.6 (case a), 0.4 (case b), and 0.2 (case c); car and quadricycle charge powers taken into account are shown in the first and in the second row on the category axis, respectively.

Fig. 6 shows the self-consumption in case of contemporary charge of two quadricycles, considering the values of ΔSOC form 0.2 to 0.6 as reported on the category axis.

B. Scenario 2: Sequential Charging

The second set of graphs (Figs. 7–9) shows the results obtained for the sequential charging scenario. The same combinations of vehicles, charging power, and ΔSOC considered in the scenario 1 are taken into account. In the case of sequential charging with different recharging power or with different energy demand, each case has to be considered twice because the order of recharge has to be taken into account. Fig. 7 shows the self-consumption in case of sequential charge of two cars, considering the values of ΔSOC of 0.6 (case a), 0.4 (case b), and 0.2 (case c). Fig. 8 shows the self-consumption

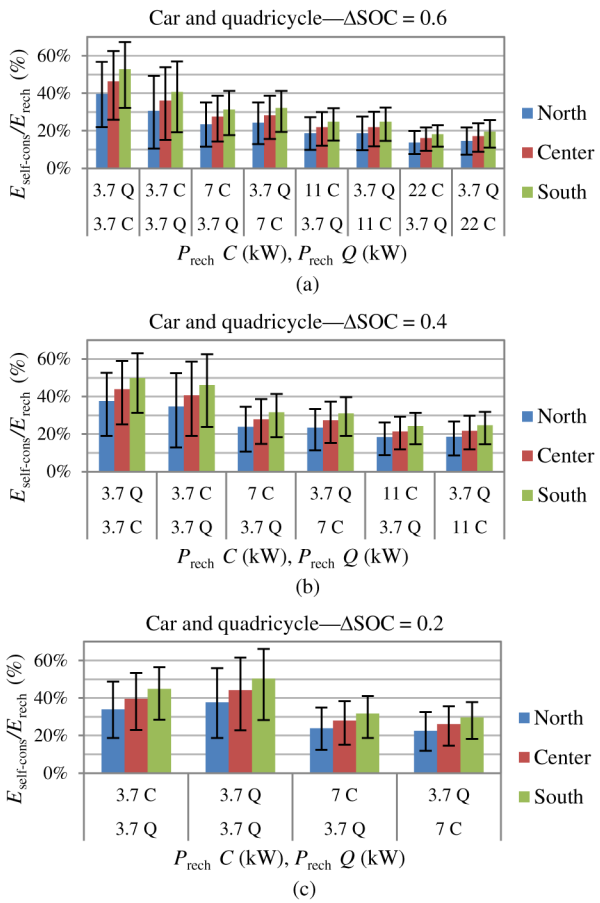

Fig. 8. (a) $\Delta SOC = 0.6$. (b) $\Delta SOC = 0.4$. (c) $\Delta SOC = 0.2$. Sequential charging of a cars and a quadricycle. The recharge power of the car (C) and quadricycle (Q) are reported on the category axis.

in case of contemporary charge of a car and a quadricycle, considering the values of ΔSOC of 0.6 (case a), 0.4 (case b), and 0.2 (case c). Fig. 9 shows the self-consumption in case

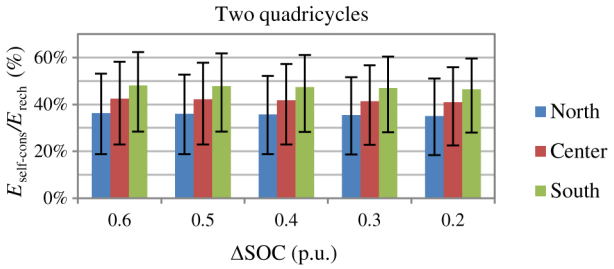

Fig. 9. Sequential charging of two quadricycles. The ΔSOC of each quadricylce are reported on the category axis.

of contemporary charge of two quadricycles, considering the values of ΔSOC form 0.2 to 0.6.

C. Comments on the Results

A first analysis of these values shows that only a small proportion of energy produced from PV can be supplied directly into the electric vehicle batteries. The sequential charging allows a self-consumption higher than the simultaneous charging. This increase steps around 10%–15% points and is far from taking a double absorption value (except in the case of the two quadricycle). This effect penalizes, especially in the winter months. For both types of recharging, the combination of car and quadricycle, with maximum ΔSOC and minimum charging power presents the most favorable case. The combination of two cars with a maximum charging power of 22 kW is the most unfavorable case regarding. For both types of recharging, the combination of car and quadricycle with maximum ΔSOC and minimum charging power presents the most favorable case. The combination of two cars, with a maximum charging power of 22 kW is the most unfavorable case regarding. In fact, because the peak power of the PV shelter is equal to 3.7 kW and the maximum average power is slightly higher than 2.6 kW, it is evident that, by requiring more charging power, most of the energy is drawn from the grid.

The combination of two quadricycles is the case that takes greater advantage in moving from simultaneous to sequential charging. In fact, the sequential recharge shifts the second vehicle in the time slot that starts at 13.30, when the PV production is higher; therefore, it is possible to have a better exploitation of the renewable source. In the case of simultaneous charging, there are groups of different scenarios that lead to the same results. In particular, the self-consumption (at equal ΔSOC) depends only on the lower charging power considered for the particular scenario. Since the power from PV generator is always lower than the minimum power required for charging one EV, the charging time depends only on the lower power considered for charging one EV.

It can be concluded that the most important aspect to maximize the self-consumption, useful to maximize the payback time of the PV shelter, is to spread the EVs recharge during the maximum production periods of PV system. This is possible only if there are no time constraints, such as in a situation of working periods.

VI. Conclusion

This paper aims to examine the potential and the technical benefits of using PV systems as energy supplier for charging PHEV. For this purpose, first, suitable mathematical functions have been developed to estimate the energy production from PV systems in different geographical locations in Italy as a function of tilt, azimuth, and month.

Successively, to determine the strategy that maximizes the self-consumption recharging with the lowest power, a PV carport combined with a charging system for two electric cars has been analyzed. The aspects linked to the energy flows, considering the production of PV system, the absorption by charging EVs, and the absorbed and injected energy to the utility grid are evaluated, highlighting the technical sustainability of the project. The comparability between the values of the energy produced by PV and the one demanded by the PHEVs is difficult to obtain due to the noncoordination of the solar source and the load.

Different scenarios and more than 9000 cases are analyzed in terms of absorption profiles and energy. The most significant results of this work is the percentage of energy coming from the PV system to the EVs with respect to the energy required by the charging point, that ranges from 1%–3% to 56%–72%. Moreover, the energy flows strongly depend on month. The maximization of the energy flow from PV system to electric vehicle requires quite long and low power charges that allow exploiting the hours when production of the PV shelter is high. However, an energy storage system is necessary.

References

[1] J. Widén, "Correlations between large-scale solar and wind power in a future scenario for Sweden," *IEEE Trans. Sustain. Energy*, vol. 2, no. 2, pp. 177–184, Apr. 2011.

[2] S. Rezaee, E. Fariah, and B. Khorramdel, "Probabilistic analysis of plug-in electric vehicles impact on electrical grid through homes and parking lots," *IEEE Trans. Sustain. Energy*, vol. 4, no. 4, pp. 1024–1033, Oct. 2013.

[3] U. C. Chukwu and S. M. Mahajan, "V2G parking lot with PV rooftop for capacity enhancement of a distribution system," *IEEE Trans. Sustain. Energy*, vol. 5, no. 1, pp. 119–127, Jan. 2014.

[4] Z. Darabi and M. Ferdowsi, "Aggregated impact of plug-in hybrid electric vehicles on electricity demand profile," *IEEE Trans. Sustain. Energy*, vol. 2, no. 4, pp. 501–508, Oct. 2011.

[5] M. Falahi, H.-M Chou, M. Ehsani, L. Xie, and K. L. Butler-Purry, "Potential power quality benefits of electric vehicles," *IEEE Trans. Sustain. Energy*, vol. 4, no. 4, pp. 1016–1023, Oct. 2013.

[6] L. Cheng, Y. Chang, J. Lin, and C. Singh, "Power system reliability assessment with electric vehicle integration using battery exchange mode," *IEEE Trans. Sustain. Energy*, vol. 4, no. 4, pp. 1034–1042, Oct. 2013.

[7] X. Li, L. A. C. Lopes, and S. S. Williamson, "On the suitability of plug-in hybrid electric vehicle (PHEV) charging infrastructures based on wind and solar energy," in *Proc. Power Energy Soc. Gen. Meeting*, 2009, pp. 1–8.

[8] M. Brenna, F. Foiadelli, M. Roscia, and D. Zaninelli, "Synergy between renewable sources and electric vehicles for energy integration in distribution systems," in *Proc. 15th IEEE Int. Conf. Harmonics Qual. Power (ICHQP)*, 2012, pp. 865–869.

[9] Y. Zong *et al.*, "Model predictive controller for active demand side management with PV self-consumption in an intelligent building," in *Proc. 3rd IEEE PES Int. Conf. Exhib. Innovative Smart Grid Technol. (ISGT Eur.)*, 2012, pp. 1–8.

[10] D. Carli, M. Ruggeri, M. Bottarelli, and M. Mazzer, "Grid-assisted photovoltaic power supply to improve self-sustainability of ground-source heat pump systems," in *Proc. IEEE Int. Conf. Ind. Technol. (ICIT)*, 2013, pp. 1579–1584.

[11] M. Brenna, F. Foiadelli, and D. Zaninelli, "Integration of recharging infrastructures for electric vehicles in urban transportation system," in *Proc. 2nd IEEE Int. Energy Conf. Exhib. (ENERGYCON)*, 2012, pp. 1060–1064.
[12] A. Dolara, G. C. Lazaroiu, S. Leva, and G. Manzolini, "Experimental investigation of partial shading scenarios on PV (photovoltaic) modules," *Energy*, vol. 55, no. 15, pp. 466–475, 2013.
[13] M. Brenna, A. Dolara, F. Foiadelli, G. C. Lazaroiu, and S. Leva, "Transient analysis of large scale PV systems with floating dc section," *Energies*, vol. 5, no. 10, pp. 3736–3752, 2012.
[14] E. Ogliari, F. Grimaccia, S. Leva, and M. Mussetta, "Hybrid predictive models for accurate forecasting in PV systems," *Energies*, vol. 6, no. 4, pp. 1918–1929, 2013.
[15] A. Ashtari, E. Bibeau, S. Shahidinejad, and T. Molinski, "PEV charging profile prediction and analysis based on vehicle usage data," *IEEE Trans. Smart Grid*, vol. 3, no. 1, pp. 341–350, Mar. 2012.
[16] S. Shahidinejad, E. Bibeau, and S. Filizadeh, "Statistical development of a duty cycle for plug-in vehicles in a North American urban setting using fleet information," *IEEE Trans. Veh. Technol.*, vol. 59, no. 8, pp. 3710–3719, Oct. 2010.
[17] (2013). *Software Photovoltaic Geographical Information System* [Online]. Available: http://re.jrc.ec.europa.eu/pvgis